Inorganica Chimica Acta 399 (2013) 138–145

Contents lists available at SciVerse ScienceDirect

Inorganica Chimica Acta

journal homepage: www.elsevier.com/locate/ica

fac-Tricarbonyl rhenium(I) complexes of 2-(alkylthio)-N-((pyridine-2-yl)methylene)benzenamine: Synthesis, spectroscopic characterization, X-ray structure and DFT calculation

Mahendra Sekhar Jana, Ajoy Kumar Pramanik, Subhankar Kundu, Deblina Sarkar, Tapan Kumar Mondal *

Inorganic Chemistry Section, Department of Chemistry, Jadavpur University, Kolkata 700032, India

ARTICLE INFO

Article history:
Received 31 March 2012
Received in revised form 3 January 2013
Accepted 4 January 2013
Available online 26 January 2013

Keywords:
Re(I) carbonyl complex
X-ray structure
Electrochemistry
Photophysical property
DFT calculation

ABSTRACT

The paper presents a combined experimental and computational study of tricarbonyl complexes *fac*-[Re(CO)$_3$(L^1/L^2)Cl] (**1a/1b**) (L^1 = 2-(methylthio)-N-((pyridine-2-yl)methylene)benzenamine and L^2 = 2-(ethylthio)-N-((pyridine-2-yl)methylene)benzenamine). The Schiff base ligands **L^1** and **L^2** have been synthesized and characterized by elemental and spectroscopic analysis. Along with spectral characterizations, the structural confirmation by single crystal X-ray study has been done for complex **1a**. The rhenium atom adopts a distorted octahedral geometry and is coordinated by three carbonyl ligands in a *fac* arrangement. The electronic structure, redox properties, absorption and emission properties of ligands and complexes have been explained based on DFT and TDDFT calculations. The complexes show MLCT bands at 443–448 nm and emitted at 405–410 nm upon excitation at 320–326 nm, characterized as ILCT transitions.

1. Introduction

The transition metal complexes having π-acidic diimine (–N=C–C=N–) functional polypyridyl ligands display exciting photochemical and photophysical properties, and have application in many technological fields [1–4]. The excited states of these compounds are often sufficiently long-lived to become engaged in energy transfer reactions. Their electroluminescent properties have been applied in solar energy converters [5], as electroluminescent materials in OLED-type devices [4,6–11], and, particularly as luminescent probes for long-range electron-transfer studies in proteins and other biomolecular systems [12–14], and light-emitting electronic devices [15,16]. The photochemistry and photochemical properties of rhenium tricarbonyl complexes with this type of ligands were extensively studied by D.J. Stufkens in the 90's [17–19]. Interest in this type of photoluminescent compounds remains strong as evidenced by a number of recent reviews [6,20,21]. Study of the redox properties of these compounds can yield insight into their photophysical and photochemical properties [22–25].

Chelating ligands containing N,N,S donor atoms have unique interest in the coordination chemistry because of the stability, chemical and electrochemical activities and diversity in binding to metal ions [26–33]. In recent years, several groups have used polydentate ligands with thioether moieties for the synthesis of model complexes to mimicking the spectroscopic and structural properties of the active sites of metallo proteins [34–37]. In this work we have synthesized the *fac*-[Re(CO)$_3$(L^1/L^2)Cl] (**1a/1b**) complexes with thioether containing Schiff base ligands **L^1** and **L^2** (where L^1 = 2-(methylthio)-N-((pyridine-2-yl)methylene)benzenamine and L^2 = 2-(ethylthio)-N-((pyridine-2-yl)methylene)benzenamine). The characterization of *fac*-[Re(CO)$_3$(L^1/L^2)Cl] (**1a/1b**) were carried out by spectral and elemental analysis, and the structure has been confirmed by single crystal X-ray structure for complex **1a**. The electronic transitions, assignment of spectral bands and redox properties have been explained based on DFT and TDDFT calculations.

2. Experimental

2.1. Materials

2-(Alkylthio)thiobenzenamine was prepared following the published procedure [38]. Pyridine-2-carboxaldehyde, 2-aminothiophenol and Re(CO)$_5$Cl were purchased from Aldrich, and used as received. All other chemicals and solvents were of reagent grade and were used without further purification.

2.2. Physical measurements

Microanalyses (C, H, N) were performed using a Perkin-Elmer CHN-2400 elemental analyzer. The electronic spectra were mea-

* Corresponding author. Fax: +91 033 24146584.
E-mail address: tkmondal@chemistry.jdvu.ac.in (T.K. Mondal).

0020-1693/$ - see front matter © 2013 Elsevier B.V. All rights reserved.
http://dx.doi.org/10.1016/j.ica.2013.01.013

sured on Lambda 25 Perkin Elmer spectrophotometer in acetonitrile solution. The IR spectra were recorded on RX-1 Perkin Elmer spectrophotometer in the spectral range 4000–400 cm^{-1} with the samples in the form of KBr pellets. Luminescence property was measured using LS-55 Perkin Elmer fluorescence spectrophotometer at room temperature (298 K) in acetonitrile solution by 1 cm path length quartz cell. Fluorescence lifetimes were measured using a time-resolved spectrofluorometer from IBH, UK. The instrument uses a picoseconds diode laser (NanoLed-03, 370 nm) as the excitation source and works on the principle of time-correlated single photon counting [39]. The goodness of fit was evaluated by χ^2 criterion and visual inspection of the residuals of the fitted function to the data. ^{1}H NMR spectra were recorded in $CDCl_3$ on Bruker 300 MHz FT-NMR spectrometers in presence of TMS as internal standard. Cyclic voltammetric measurements were carried out using a CH1 Electrochemical workstation. A platinum wire working electrode, a platinum wire auxiliary electrode and Ag/AgCl reference electrode were used in a standard three-electrode configuration. [nBu$_4$N][ClO_4] was used as the supporting electrolyte and the scan rate used was 50 mV s^{-1} in acetonitrile under dinitrogen atmosphere. The reported potentials are uncorrected for junction potential.

The luminescence quantum yield was determined using carbazole as reference with a known ϕ_R of 0.42 in MeCN. The complex and the reference dye were excited at the same wavelength, maintaining nearly equal absorbance (~0.1), and the emission spectra were recorded. The area of the emission spectrum was integrated using the software available in the instrument and the quantum yield is calculated according to the following equation:

$$\phi_S/\phi_R = [A_S/A_R] \times [(Abs)_R/(Abs)_S] \times [\eta_S^2/\eta_R^2]$$

Here, ϕ_S and ϕ_R are the luminescence quantum yield of the sample and reference, respectively. A_S and A_R are the area under the emission spectra of the sample and the reference respectively, $(Abs)_S$ and $(Abs)_R$ are the respective optical densities of the sample and the reference solution at the wavelength of excitation, and η_S and η_R are the values of refractive index for the respective solvent used for the sample and reference.

2.3. Synthesis of complexes

2.3.1. Preparation of ligands (**L^1**/**L^2**)

2-(Methylthio)benzenamine (210 mg, 0.66 mmol) and pyridine-2-carboxaldehyde (72 mg, 0.67 mmol) were refluxed for 10 h in dry ethanol. The reaction mixture was cooled and solvent was removed under reduced pressure. The gummy mass of L^1 so obtained was thoroughly washed with *n*-hexane. Yield was 123 mg, 82%.

Ligand L^2 was synthesized following the same procedure of L^1. Yield was 80%.

Anal. Calc. for $C_{13}H_{12}N_2S$ (**L^1**): C, 68.39; H, 5.30; N, 12.27. Found: C, 68.46; H, 5.31; N, 12.30%. IR data (KBr, cm^{-1}): 1622 ν(C=N). ^{1}H NMR data ($CDCl_3$, ppm): 8.76 (1H, d, J = 4.1 Hz), 8.40 (1H, d, J = 8.0), 7.82 (2H, m), 7.55 (1H, t, J = 8.2 Hz), 7.18 (2H, m), 6.78 (2H, t, J = 8.0 Hz), 2.67 (3H, s).

Anal. Calc. for $C_{14}H_{14}N_2S$ (**L^2**): C, 69.39; H, 5.82; N, 11.56. Found: C, 69.44; H, 5.81; N, 11.58%. IR data (KBr, cm^{-1}): 1625 ν(C=N). ^{1}H NMR data ($CDCl_3$, ppm): 8.70 (1H, d, J = 3.8 Hz), 8.38 (1H, d, J = 7.9), 7.85 (2H, m), 7.51 (1H, t, J = 8.1 Hz), 7.16 (2H, m), 6.71 (2H, t, J = 8.2 Hz), 2.98 (2H, q, J = 7.4 Hz), 1.37 (3H, t, J = 7.4 Hz).

2.3.2. Preparation of [Re(CO)$_3$(L^1/L^2)Cl] (**1a**/**1b**)

$Re(CO)_5Cl$ (100 mg, 0.27 mmol) and L^1 (63 mg, 0.28 mmol) in toluene (50 ml) were refluxed for 4 h. The resulting reaction mixture was allowed to cool to room temperature. After removal of the solvent in reduced pressure the crude product was purified by column chromatography on neutral alumina using toluene and acetonitrile mixture (v:v, 3:1) as eluent. The solvent mixture was removed in reduced pressure to obtain brown solid of **1a**. Yield was 107 mg, 74%.

Complex **1b** was synthesized following the same procedure as of **1a**. Yield was 69%.

Anal. Calc. for $C_{16}H_{12}ClN_2O_3ReS$ (**1a**): C, 35.99; H, 2.27; N, 5.25. Found: C, 35.85; H, 2.26; N, 5.23%. IR data (KBr, cm^{-1}): 2018, 1913 ν(CO); 1589 ν(C=N). ^{1}H NMR data ($CDCl_3$, ppm): 8.87 (1H, d, J = 4.0 Hz), 8.52 (1H, d, J = 8.0), 7.97 (2H, m), 7.69 (1H, t, J = 8.1 Hz), 7.21 (2H, m), 6.83 (2H, t, J = 8.0 Hz), 2.83 (3H, s). E_{pa} (Re^I/Re^{II}): 1.15 V; E_{pc}: −1.12 V.

Anal. Calc. for $C_{17}H_{14}ClN_2O_3ReS$ (**1b**): C, 37.26; H, 2.57; N, 5.11. Found: C, 37.16; H, 2.57; N, 5.09%. IR data (KBr, cm^{-1}): 2020, 1916 ν(CO); 1595 ν(C=N). ^{1}H NMR data ($CDCl_3$, ppm): 8.92 (1H, d, J = 3.8 Hz), 8.53 (1H, d, J = 8.0), 7.93 (2H, m), 7.66 (1H, t, J = 8.0 Hz), 7.19 (2H, m), 6.80 (2H, t, J = 7.9 Hz), 3.13 (2H, q, J = 7.6 Hz), 1.41 (3H, t, J = 7.5 Hz). E_{pa} (Re^I/Re^{II}): 1.12 V; E_{pc}: −1.15 V.

2.4. Computational details

Full geometry optimization was carried out using the density functional theory method at the B3LYP level for the representative complex **1a** [40,41]. All elements except rhenium were assigned the 6-31G(d) basis set. The SDD basis set with effective core potential was employed for the rhenium atom [42,43]. The vibrational frequency calculation was performed to ensure that the optimized geometry represents the local minima and there are only positive eigenvalues. All calculations were performed with GAUSSIAN03 program package [44] with the aid of the GaussView visualization program. Natural bond orbital analyses were performed using the NBO 3.1 module of GAUSSIAN03. Vertical electronic excitations based on B3LYP optimized geometry were computed using the time-dependent density functional theory (TDDFT) formalism [45–47] in acetonitrile using conductor-like polarizable continuum model (CPCM) [48–50]. GaussSum [51] was used to calculate the fractional contributions of various groups to each molecular orbital.

2.5. Crystal structure determination and refinement

Details of crystal analysis, data collection and structure refinement data for **1a** is given in Table 1. Crystal mounting was done on glass fibers with epoxy cement. Single crystal data collections were performed with an automated Bruker SMART APEX CCD diffractometer using graphite monochromatized Mo Kα radiation (λ = 0.71073 Å). Reflection data were recorded using the ω scan technique. Unit cell parameters were determined from least-squares refinement of setting angles with θ in the range $1.84 \leqslant \theta \leqslant 25.00°$. Out of 11918 collected data 2956 with $I > 2\sigma(I)$ were used for structure solution within *hkl* parameters $-9 \leqslant h \leqslant 9$, $-11 \leqslant k \leqslant 11$, $-13 \leqslant l \leqslant 12$. The structures were solved and refined by full-matrix least-squares techniques on F^2 using the SHELXS-97 program [52]. The absorption corrections were done by the multi-scan technique. All data were corrected for Lorentz and polarization effects, and the non-hydrogen atoms were refined anisotropically. Hydrogen atoms were generated using SHELXL-97 [53] and their positions calculated based on the riding mode with thermal parameters equal to 1.2 times that of the associated C atoms, and participated in the calculation of the final *R*-indices.

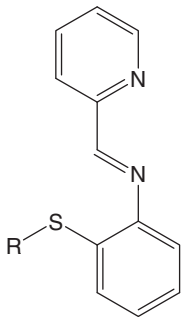

2-(Alkylthio)-N-((pyridin-2-yl) methylene)benzenamine
Where, R = Me (**L^1**) and Et (**L^2**)

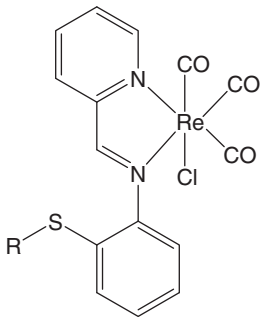

fac-[Re(CO)$_3$(L^1/L^2)Cl] (1a/**1b**)

Scheme 1. Structure of ligands (**L^1**/**L^2**) and *fac*-[Re(CO)$_3$(L^1/L^2)Cl] (**1a**/**1b**) complexes.

Table 1
Crystallographic data and refinement parameters for **1a**.

Empirical formula	$C_{16}H_{12}ClN_2O_3ReS$
Formula weight	533.99
Crystal system	triclinic
Space group	$P\bar{1}$
a (Å)	8.1877(2)
b (Å)	9.9841(3)
c (Å)	11.1123(3)
α (°)	84.575(2)
β (°)	86.105(2)
γ (°)	70.027(2)
V (Å^3)	849.32(4)
Z	2
ρ_{calcd} (g cm^{-3})	2.088
μ (mm^{-1})	7.450
T (K)	293(2)
hkl range	−9–9, −11–11, −13–12
F(000)	508
θ range (°)	1.84 to 25.00
Reflections collected	11918
Unique reflections (R_{int})	2956 [0.0352]
Observed data ($I > 2\sigma(I)$)	2558
Data/restraints/parameters	2956/0/205
R_1[a], wR_2[b] ($I > 2\sigma(I)$)	0.0644, 0.1664
R_1, wR_2 (all data)	0.0746, 0.1739
Goodness-of-fit (GOF) on F^2[c]	1.040
Largest difference in peak and hole (e Å^{-3})	2.101 and −1.434

[a] $R_1 = \sum||F_o| - |F_c||/\sum|F_o|$.
[b] $wR_2 = \{\sum[w(F_o^2 - F_c^2)^2]/\sum[w(F_o^2)^2]\}^{1/2}$, $w = 1/[\sigma^2(F_o^2) + (0.1123\ P)^2 + 8.6320\ P]$, where $P = (F_o^2 + 2\ F_c^2)/3$.
[c] GOF = $\{\sum[w(F_o^2 - F_c^2)^2]/(n-p)\}^{1/2}$, where n = number of measured data and p = number of parameters.

Table 3
Some selected bond distances (Å) and angles (°) of **1a**.

Bond distance (Å)	X-ray	Calc.
Re(1)–Cl(1)	2.457(4)	2.499
Re(1)–N(1)	2.149(10)	2.196
Re(1)–N(2)	2.164(12)	2.210
Re(1)–C(14)	1.904(17)	1.913
Re(1)–C(15)	1.925(16)	1.932
Re(1)–C(16)	1.901(19)	1.926
C(14)–O(1)	1.110(18)	1.158
C(15)–O(2)	1.120(18)	1.149
C(16)–O(3)	1.13(2)	1.152
Angles (°)		
N(1)–Re(1)–Cl(1)	84.1(3)	82.79
N(1)–Re(1)–N(2)	73.1(4)	74.41
N(1)–Re(1)–C(14)	94.6(5)	94.55
N(1)–Re(1)–C(15)	171.2(5)	171.1
N(1)–Re(1)–C(16)	100.5(6)	98.05
N(2)–Re(1)–Cl(1)	81.3(3)	83.54
N(2)–Re(1)–C(14)	96.8(5)	94.29
N(2)–Re(1)–C(15)	98.6(6)	98.49
N(2)–Re(1)–C(16)	171.9(6)	170.9
C(14)–Re(1)–Cl(1)	178.0(4)	177.3
C(14)–Re(1)–C(15)	89.4(6)	91.17
C(14)–Re(1)–C(16)	88.5(6)	90.06
C(15)–Re(1)–Cl(1)	91.7(4)	91.43
C(15)–Re(1)–C(16)	87.5(7)	89.06
Re(1)–C(14)–O(1)	177.1(14)	179.6
Re(1)–C(15)–O(2)	179.5(16)	179.0
Re(1)–C(16)–O(3)	177.3(14)	177.8

3. Results and discussion

3.1. Synthesis and formulation

The *fac*-[Re(CO)$_3$(L^1/L^2)Cl] (**1a/1b**) complexes were prepared by the reaction of Re(CO)$_5$Cl with Schiff base ligands **L^1** and **L^2** (where, L^1 = 2-(methylthio)-N-((pyridine-2-yl)methylene)benzenamine and L^2 = 2-(ethylthio)-N-((pyridine-2-yl)methylene)benzenamine) in toluene under refluxing condition in 1:1 ratio. The structures of the ligands and the complexes having general formula *fac*-[Re(CO)$_3$(L^1/L^2)Cl] (**1a**/**1b**) are shown in Scheme 1. In the course of reaction two CO groups were replaced by pyridine-N and imine-N donor centers of the ligand. Characterizations of ligands and complexes were carried out by IR, NMR, UV–Vis and elemental analysis. In the IR spectra, two typical bands around 2018–2020 and 1913–1916 cm^{-1} are observed (Calculated (scaling factor 0.97), 2024, 1952, 1918 cm^{-1} for **1a**), which correspond to the *fac*-Re(CO)$_3$ fragment in the complexes. The ν(C=N) stretching in the complexes are observed at around 1589–1595 cm^{-1}. The ν(C=N) for free ligands are observed at 1622–1625 cm^{-1}, which is significantly shifted to lower frequency region in the complexes supporting coordination of imine-N (Table 2). The ^{1}H NMR spectra

Table 2
FT-IR, UV–Vis, emission and life time data of ligands (**L^1** and **L^2**) and complexes (**1a** and **1b**).

Compd.	ν(CO) (cm^{-1})[a]	λ_{max} (M^{-1} cm^{-1})[b]	Emission[b]			Life time[b]	
			λ_{ex} (nm)	λ_{em} (nm)	ϕ	χ^2	τ_f (ns)[c]
L^1	–	379 (4804), 321 (7027), 362(31497)	321	397	0.024	1.05	3.03
L^2	–	382 (5124), 323 (8142), 365(29435)	323	401	0.022	1.03	2.97
1a	2018, 1913	443 (5070), 326 (11728), 261 (26795)	326	405	0.013	0.98	4.49
1b	2020, 1916	448 (5642), 320 (10765), 266 (22756)	320	410	0.014	1.05	4.21

[a] KBr disk.
[b] Acetonitrile as solvent.
[c] Mean fluorescence lifetime, $\tau_f = a_1\tau_1 + a_2\tau_2$, where a_1 and a_2 are relative amplitude of decay process; $\tau_1 = 1.039$ ns, $\tau_2 = 4.532$ ns ($a_1 = 43\%$ and $a_2 = 57\%$) for **L^1**; $\tau_1 = 1.084$ ns, $\tau_2 = 4.482$ ns ($a_1 = 45\%$ and $a_2 = 55\%$) for **L^2**; $\tau_1 = 1.211$ ns, $\tau_2 = 6.349$ ns ($a_1 = 46\%$ and $a_2 = 54\%$) for **1a** and $\tau_1 = 1.946$ ns, $\tau_2 = 6.296$ ns ($a_1 = 48\%$ and $a_2 = 52\%$) for **1b**.

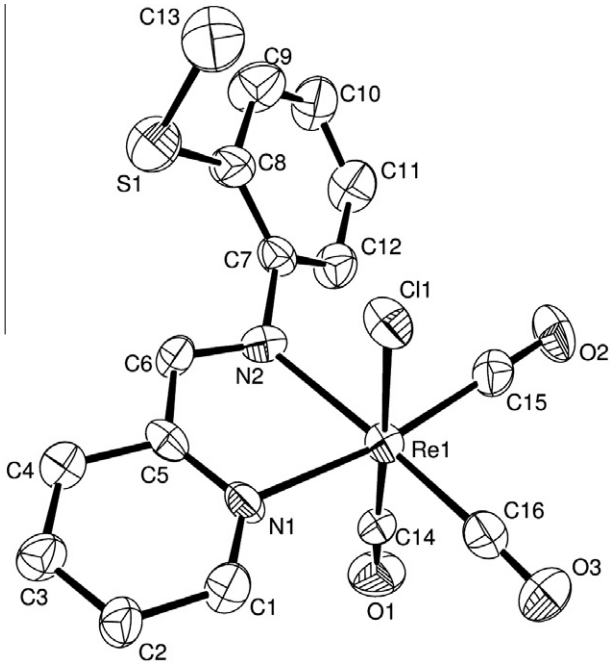

Fig. 1. Ortep structure of **1a** with 35% ellipsoidal probability.

Table 4
Energy and compositions of some selected molecular orbitals of **1a**.

MO	Energy (eV)	% Of composition			
		Re	CO	L	Cl
LUMO+5	−0.62	28	48	24	0
LUMO+4	−0.74	25	39	35	01
LUMO+3	−0.91	24	25	51	0
LUMO+2	−1.10	09	12	79	0
LUMO+1	−1.92	02	01	97	0
LUMO	−3.16	04	03	92	01
HOMO	−5.95	44	21	02	33
HOMO−1	−6.02	41	18	05	36
HOMO−2	−6.49	12	05	81 (S, 61)	02
HOMO−3	−6.58	57	23	19	01
HOMO−4	−7.11	08	04	74	14
HOMO−5	−7.29	24	08	12	56
HOMO−6	−7.40	08	03	76	13
HOMO−7	−7.51	18	05	48	29
HOMO−8	−7.93	11	12	05	72
HOMO−9	−8.46	02	01	95	02
HOMO−10	−9.03	0	0	100 (S, 45)	0

of ligands and complexes are recorded in $CDCl_3$ solution and the signals appeared as expected. The important observation is the down field shifting of pyridine protons by 0.3–0.6 ppm in the complexes compare to free ligand values supporting the coordination of pyridine-N to metal center (see Section 2).

3.2. Molecular structure

Single crystal suitable for structure determination was obtained by slow diffusion of *n*-hexane into dichloromethane solution of **1a**. The crystallographic data collection and refinement parameters are given in Table 1; selected bond lengths and angles are given in Table 3. ORTEP plot with atomic numbering scheme is shown in Fig. 1. The rhenium atom adopts a distorted octahedral geometry and is coordinated by three carbonyl ligands in a *fac* arrangement, two nitrogen atoms (pyridine-N and imine-N) of $\mathbf{L^1}$ ligand and chlorine atom. The deviation of the Rhenium coordination sphere from the ideal octahedron is because of the small bite angle of the five membered chelate ring (Re1–N1–C5–C6–N2) [73.1(4)°]. The Re–N(pyridyl) bond, Re(1)–N(1), 2.149(10) Å is shorter than the Re–N(imine), Re(1)–N(2), 2.164(12) Å. The Re–C(CO) (Re(1)–C(14), 1.904(17); Re(1)–C(15), 1.925(16) and Re(1)–C(16, 1.901(19) Å) and C–O (C(14)–O(1), 1.110(18); C(15)–O(2), 1.120(18) and C(16)–O(3), 1.13(2) Å) bond distances are found as expected for similar rhenium carbonyl complexes [54–56].

3.3. DFT calculation and electronic structure

The geometry of $\mathbf{L^1}$ and *fac*-[Re(CO)$_3$(L^2)Cl] (**1a**) were optimized in singlet state by the DFT method with the B3LYP hybrid functional. The optimized geometric parameters for **1a** are given in Table 3. The calculated bond parameters for **1a** are well correlated with the X-ray crystal structure data.

The energy and compositions of some selected molecular orbitals for **1a** are given in Table 4. Contour plots of some selected molecular orbitals of $\mathbf{L^1}$ and **1a** are presented in Fig. 2 and Fig. 3 respectively. The LUMO of L^1 have π^* character while the HOMO to HOMO−2 are π character with reduced contribution of $p\pi$(S) orbitals. The low lying virtual orbitals, LUMO to LUMO+2 correspond to π^* orbital of $\mathbf{L^1}$, while LUMO+3 to LUMO+5 show greater mixing of $d\pi$(Re) and π^*(CO) orbitals along with the contribution of L^1 for complex **1a**. The HOMO and HOMO−1 orbitals have the mixed contribution of $d\pi$(Re), $p\pi$(Cl) and π-orbitals of CO. The HOMO−2 concentrated on S atom (64% $p\pi$(S)) along with reduced contribution from $d\pi$(Re) orbitals. HOMO−3 has 57% Re($d\pi$) and reduced contribution of CO (23%).

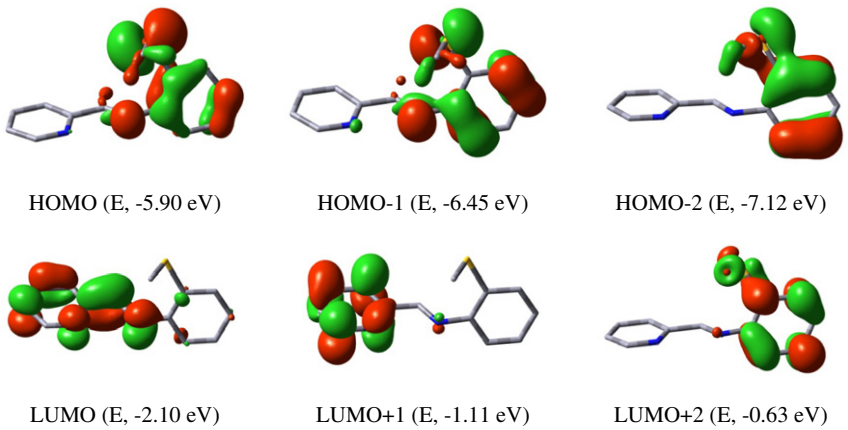

Fig. 2. Contour plot of some selected molecular orbitals of $\mathbf{L^1}$.

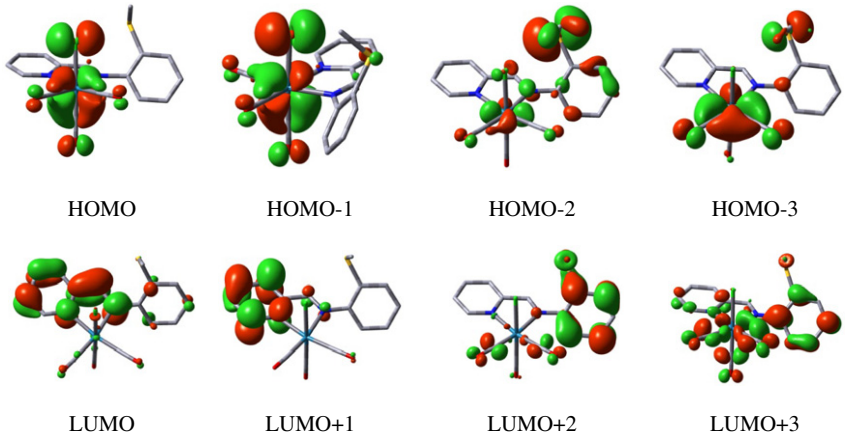

Fig. 3. Contour plot of some selected molecular orbitals of **1a**.

Table 5
Natural bond orbitals (NBOs) analysis result of **1a**.

Bonds	Occupancy	Bond orders	Contribution/hybridization	Natural charges (a.u.)	
				Atoms	Charge
Re(1)–C(14)	1.9484(0.1539)	1.3449	(37.46%)Re($sd^{2.22}$) + (62.54%)C($sp^{0.51}$)	Re(1)	−0.863
	1.7684(0.4327)		(83.72%)Re(d) + (16.28%)C(p)	Cl(1)	−0.409
	1.7205(0.4461)		(84.40%)Re(d) + (15.60%)C(p)	O(1)	−0.470
Re(1)–C(15)	1.9145(0.0874)	1.2643	(34.40%)Re($sd^{2.81}$) + (65.60%)C($sp^{0.53}$)	O(2)	−0.447
Re(1)–C(16)	1.9608(0.0984)	1.2859	(36.91%)Re($sd^{2.14}$) + (63.09%)C($sp^{0.52}$)	O(3)	−0.452
C(14)–O(1)	1.9912(0.0304)	2.0319	(30.68%)C($sp^{1.92}$) + (69.32%)O($sp^{1.33}$)	N(1)	−0.379
C(15)–O(2)	1.9970(0.0226)	2.0965	(31.26%)C($sp^{1.96}$) + (68.74%)O($sp^{1.29}$)	N(2)	−0.368
	1.9962(0.2525)		(24.36%)C(p) + (75.64%)O(p)	C(14)	0.670
	1.9951(0.2206)		(24.86%)C(p) + (75.14%)O(p)	C(15)	0.735
C(16)–O(3)	1.9972(0.0187)	2.0818	(31.09%)C($sp^{1.89}$) + (68.91%)O($sp^{1.25}$)	C(16)	0.727
	1.9955(0.2164)		(24.67%)C(p) + (75.33%)O(p)		
	1.9949(0.1872)		(24.86%)C(p) + (75.14%)O(p)		

To understand the nature of Re–CO bonding the natural bond orbitals (NBOs) calculation has been performed on the optimized structure of **1a**. The occupancies and hybridizations of the calculated Re–C and C–O natural bond orbitals (NBOs) are summarized in Table 5. For each carbonyl group three natural bond orbitals should be detected for the C–O bond, and one orbital for the Re–C bond [57]. But in our case the NBO analysis is found as expected for Re–CO bonds *trans* to pyridine-N and imine-N, while three natural bond orbitals for Re–C bond and one for carbonyl group *trans* to Cl are detected (Table 5). Among the three NBOs of Re–C bond *trans* to Cl, one has 37% Re and 63% C character while other two have ~84% $d\pi$(Re) contribution along with reduced contribution from C atom of carbonyl group.

The bonding between CO ligands and Re atom is supported by the resonance structure $\bar{M}—\overset{+}{C}\equiv O:$ from the calculated atomic

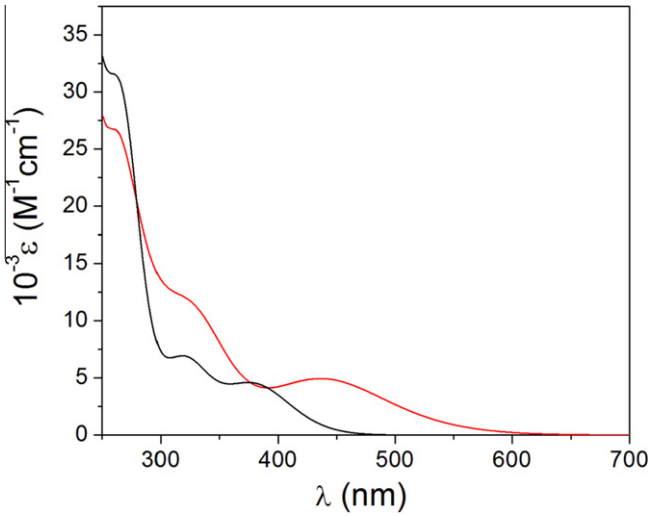

Fig. 4. UV–Vis of $\mathbf{L^1}$ (–) and **1a** (——) in acetonitrile.

Table 6
Some selected singlet–singlet vertical electronic transitions of $\mathbf{L^1}$.

Key excitations	Character	λ (nm)	*E* (eV)	Osc. strength (f)
(95%)HOMO → LUMO	$p\pi$(S) → L(π^*)	391.0	3.1709	0.0573
(94%)HOMO−1 → LUMO	L(π) → L(π^*)	331.5	3.7407	0.0839
(67%)HOMO−2 → LUMO	L(π) → L(π^*)	270.9	4.5765	0.1416
(89%)HOMO−3 → LUMO	L(π) → L(π^*)	263.9	4.6987	0.2082

Table 7
Some selected singlet–singlet vertical electronic transitions of **1a**.

Key excitations	Character	λ (nm)	*E* (eV)	Osc. strength (f)
(88%)HOMO → LUMO	$d\pi$(Re)/ Cl → L(π^*)	451.6	2.7457	0.0698
(82%)HOMO−3 → LUMO	$d\pi$(Re) → L(π^*)	406.9	3.0470	0.0251
(91%)HOMO−4 → LUMO	L(π) → L(π^*)	354.9	3.4934	0.2200
(75%)HOMO−4 → LUMO+1	L(π) → L(π^*)	266.2	4.6573	0.1613

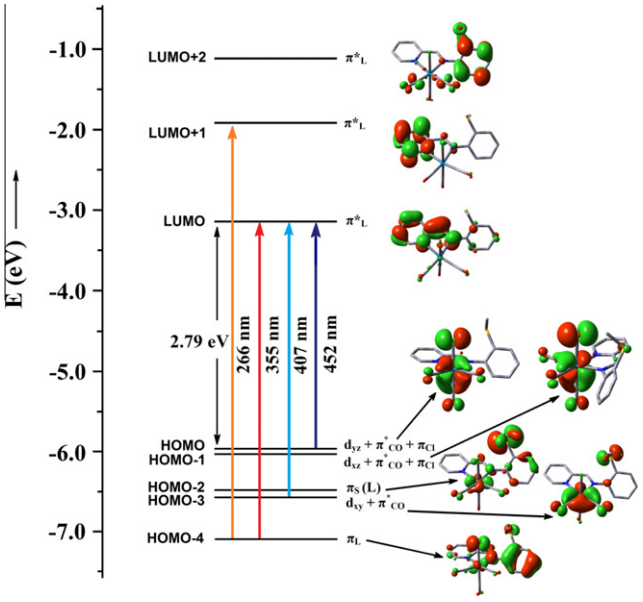

Fig. 5. Energy level diagram of MOs involved in singlet–singlet vertical excitations.

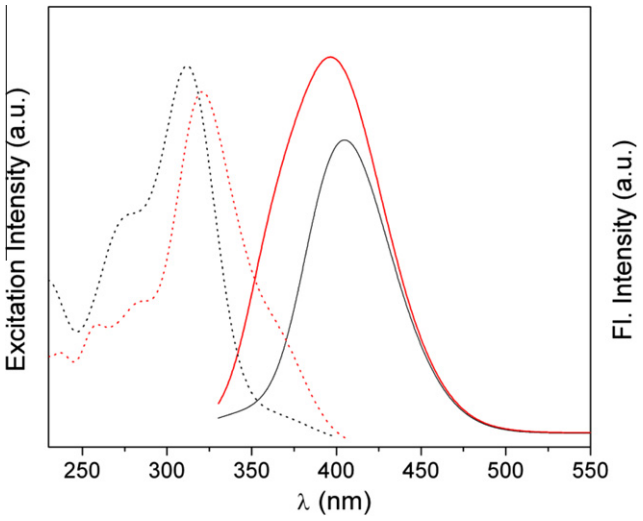

Fig. 6. Excitation and emission spectra of $\mathbf{L^1}$ (–) and **1a** (——) in acetonitrile.

charges (Table 5). The calculated natural charges on the carbon atoms of the carbonyl ligands are positive, whereas the oxygen atoms are negatively charged. The least positively charged carbon of CO groups is in the *trans* position to the halogen atom as expected. The calculated charge on the rhenium atom (−0.863 a.u.) is considerably lower than the formal charge +1. The population of the $5d_{xy}$, $5d_{xz}$, $5d_{yz}$, $5d_{x^2-y^2}$ and $5d_{z^2}$ of the rhenium atom is 1.1695, 1.4150, 1.2881, 1.4299 and 1.3146.

3.4. TD DFT calculation and electronic spectra

The $\mathbf{L^1}$ and $\mathbf{L^2}$ exhibit moderately intense absorption bands at 379–382 nm and 321–323 nm along with a shoulder at 262–265 nm. The complexes (**1a**/**1b**) show one moderately intense broad band at 443–448 nm along with an intense peak at 320–326 nm and a shoulder at 261–266 nm in acetonitrile (Table 2, Fig. 4).

To assign the nature of electronic transitions in the compounds TDDFT calculations on the optimized geometry of $\mathbf{L^1}$ and **1a** were performed in implicit acetonitrile. The bands at 379–382 nm for the ligands has been assigned as $p\pi(S) \rightarrow L(\pi^*)$ transitions, while the bands at 321–323 nm and 262–265 nm have $\pi \rightarrow \pi^*$ character (Table 6). The calculated vertical electronic transitions for **1a** show two weak transitions at 452 nm and 407 nm corresponding to HOMO → LUMO and HOMO−3 → LUMO transitions having $d\pi(Re) \rightarrow \pi^*(L)$ character along with reduced contribution of $p\pi(Cl) \rightarrow \pi^*(L)$ transitions (Table 7, Fig. 5). The high energy bands at 320–326 nm and 261–266 nm are $\pi(L) \rightarrow \pi^*(L)$, intra-ligand charge transfer (ILCT) transitions.

The ligands ($\mathbf{L^1}$/$\mathbf{L^2}$) exhibit intense emission at 397–401 nm upon excitation at 321–323 nm. For complexes (**1a**/**1b**) the emission occurs at higher energy (405–410 nm) than the lowest absorption band (443–448 nm). It would indicate the presence of a ligand-localized excited state completely decoupled from the rest of the complex. We do not observe emission upon excitation in MLCT band at 443–448 nm for the complexes. So, the $\pi(L) \rightarrow \pi^*(L)$ transitions are taken to investigate the emission properties (Table 2, Fig. 6). The emission quantum yields (ϕ) of the compounds are in the range 0.013–0.024.

Lifetime data of the compounds are taken at 298 K in acetonitrile solution when excited at 370 nm. The fluorescence decay curve was deconvoluted with respect to the lamp profile. The observed florescence decay fits with bi-exponential nature for both the ligands and complexes (Table 2, Fig. 7). We have used mean fluorescence lifetime ($\tau_f = a_1\tau_1 + a_2\tau_2$, where a_1 and a_2 are relative

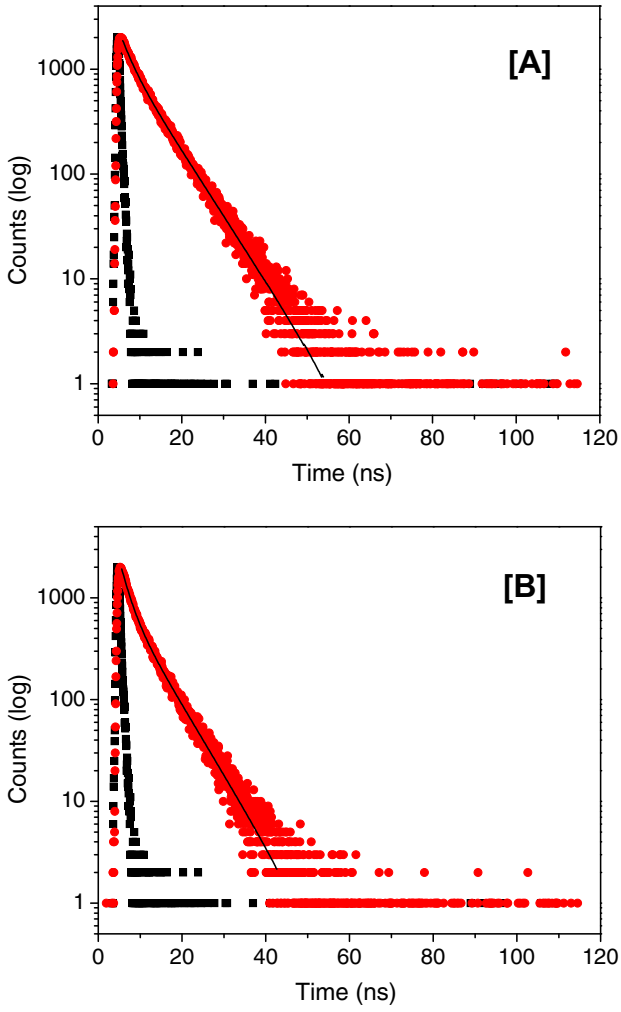

Fig. 7. Exponential decay profile of (A) ligand, $\mathbf{L^1}$ and (B) *fac*-$[Re(CO)_3(L^1)Cl]$ (**1a**) in acetonitrile.

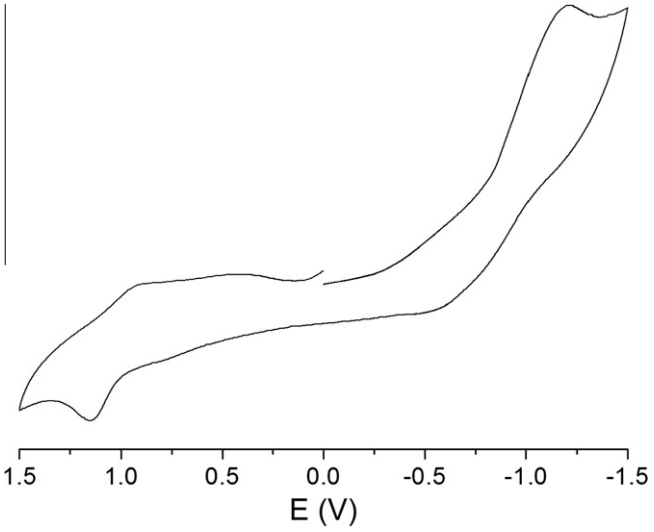

Fig. 8. Cyclic voltammogram of **1a** in acetonitrile.

amplitude of decay process) to study the excited state stability of the complexes. The fluorescence lifetime of the ligands is in the range 2.97–3.03 ns and for complexes 4.21–4.49 ns.

3.5. Electrochemistry

The complexes show one irreversible oxidative response at 1.12–1.15 V when scanned in the potential range 0.0 to 2.0 V which is assigned as Re(II)/Re(I) oxidation as HOMO of **1a** has 44% contribution of Re($d\pi$) orbitals (Fig. 8). In addition one irreversible reduction peak at around −(1.19–1.22) V has been observed for the complexes. The LUMO of complex **1a** has 92% π^*(L) character and the reduction is assigned as ligand centered. The nature of voltammogram does not change with scan rate (50–250 mV S^{-1}).

4. Conclusion

New pyridyl Schiff base ligands ($\mathbf{L^1}$/$\mathbf{L^2}$) containing thioether group have been synthesized and characterized. The rhenium carbonyl complexes containing the $\{Re(CO)_3\}^+$ fragment and Schiff base ligands ($\mathbf{L^1}$/$\mathbf{L^2}$) with general formula *fac*-[$Re(CO)_3(L^1/L^2)Cl$] (**1a/1b**) have been synthesized and characterized by both experimental and theoretical studies. X-ray and IR studies confirm the facial geometry of the carbonyl ligand in the complexes. The electrochemical properties of the complexes have been examined and supported by DFT data. The spin allowed electronic transitions computed by TDDFT method have a good agreement with the experimental spectra. The ILCT based emission properties and excited state stability of the complexes have been studied by quantum yield calculation and lifetime measurement.

Acknowledgments

Financial support received from the Department of Science and Technology, New Delhi, India (No. SR/FT/CS-73/2010) is gratefully acknowledged. Special thanks to Prof. C. Sinha, Department of Chemistry, Jadavpur University, Kolkata, India for his constant help. M.S. Jana, A.K. Pramanik, S. Kundu and D. Sarkar are thankful to CSIR, New Delhi, India for fellowship.

Appendix A. Supplementary material

CCDC 867934 contains the supplementary crystallographic data for [$Re(CO)_3(L^2)Cl$] (**1a**). These data can be obtained free of charge from The Cambridge Crystallographic Data Centre via www.ccdc.cam.ac.uk/data_request/cif. Supplementary data associated with this article can be found, in the online version, at http://dx.doi.org/10.1016/j.ica.2013.01.013.

References

[1] C. Piguet, G. Bernardinelli, G. Hopfgartner, Chem. Rev. 97 (1997) 2005.
[2] U. Knof, A. von Zelewsky, Angew. Chem., Int. Ed. 38 (1999) 303.
[3] K. Kalyanasundaram, M. Grätzel, Coord. Chem. Rev. 177 (1998) 347.
[4] V. Balzani, A. Juris, M. Venturi, S. Campagna, S. Serroni, Chem. Rev. 96 (1996) 759.
[5] M. Gratzel, Energy Resources Through Photochemistry and Catalysis, Academic, New York, 1983.
[6] I.R. Farrell, A. Vlček Jr., Coord. Chem. Rev. 208 (2000) 87.
[7] A. Vogler, H. Kunkely, Coord. Chem. Rev. 200–202 (2000) 991.
[8] A. Vlček Jr., M. Busby, Coord. Chem. Rev. 250 (2006) 1755.
[9] F. Li, G. Cheng, Y. Zhao, J. Feng, S. Liu, M. Zhang, Y. Ma, J. Shen, Appl. Phys. Lett. 83 (2003) 4716.
[10] S.S. Jurisson, J.D. Lydon, Chem. Rev. 99 (1999) 2205.
[11] W.A. Volkert, T.J. Hoffman, Chem. Rev. 99 (1999) 2269.
[12] W.B. Connick, A. Di Bilio, M.G. Hill, J.R. Winkler, H.B. Gray, Inorg. Chim. Acta 240 (1995) 169.
[13] K.K.-W. Lo, K.H.-K. Tsang, W.K. Hui, N. Zhu, Chem. Commun. (2003) 2704.
[14] A.R. Dunn, W. Belliston-Bittner, J.R. Winkler, E.D. Getzoff, D.J. Stuehr, H.B. Gray, J. Am. Chem. Soc. 127 (2005) 5169.
[15] K. Wang, L. Huang, L. Gao, L. Jin, C. Huang, Inorg. Chem. 41 (2002) 3353.
[16] Z. Si, J. Li, B. Li, F. Zhao, S. Liu, W. Li, Inorg. Chem. 46 (2007) 6155.
[17] B.D. Rossenaar, D.J. Stufkens, A. Vlček Jr., Inorg. Chem. 35 (1996) 2902.
[18] B.D. Rossenaar, E. Lindsay, D.J. Stufkens, A. Vlček Jr., Inorg. Chim. Acta 250 (1996) 5.
[19] D.J. Stufkens, A. Vlček Jr., Coord. Chem. Rev. 177 (1998) 127.
[20] K.K.-W. Lo, W.-K. Hui, C.-K. Chung, K.H.-K. Tsang, T.K.-M. Lee, C.-K. Li, J.S.-Y. Lau, D.C.-M. Ng, Coord. Chem. Rev. 250 (2006) 1724.
[21] R.A. Kirgan, B.P. Sullivan, D.P. Rillema, Top. Curr. Chem. 281 (2007) 45.
[22] A. Juris, S. Campagna, I. Bidd, J.-M. Lehn, R. Ziessel, Inorg. Chem. 27 (1988) 4007.
[23] L.D. Ciana, W.J. Dressick, D. Sandrini, M. Maestri, M. Ciano, Inorg. Chem. 29 (1990) 2792.
[24] L. Wallace, D.P. Rillema, Inorg. Chem. 32 (1993) 3836.
[25] S.R. Stoyanov, J.M. Villegas, D.P. Rillema, Inorg. Chem. 41 (2002) 2941.
[26] R.A. Allred, S.A. Hufner, K. Rudzka, A.M. Arif, L.M. Berreau, Dalton Trans. (2007) 351.
[27] M.R. Malachonsk, M. Adams, N. Elia, A.L. Rheingold, R.S. Kelly, J. Chem. Soc., Dalton Trans. (1999) 2177.
[28] B. Adhikary, S. Liu, C.R. Lucas, Inorg. Chem. 32 (1993) 5957.
[29] P. Chakraborty, S.K. Chandra, A. Chakravorty, Inorg. Chem. 32 (1993) 5349.
[30] A. Karmakar, S.B. Chaoudhury, A. Chakrovorty, Inorg. Chem. 33 (1994) 6148.
[31] K. Pramanik, S. Karmakar, S.B. Choudhury, A. Chakravorty, Inorg. Chem. 36 (1997) 3562.
[32] S. Mukhopadhyay, D. Ray, J. Chem. Soc., Dalton Trans. (1995) 265.
[33] A.K. Singh, R. Mukherjee, Dalton Trans. (2005) 2886.
[34] F. Thomas, Eur. J. Inorg. Chem. (2007) 2379.
[35] L. Zhou, D. Powell, K.M. Nicholas, Inorg. Chem. 46 (2007) 7789.
[36] M. Rombach, J. Seebacher, M. Ji, G. Zhang, G. He, M.M. Ibrahim, B. Benkmil, H. Vahrenkamp, Inorg. Chem. 45 (2006) 4571.
[37] L.M. Berreau, Eur. J. Inorg. Chem. (2006) 273.
[38] M.K. Paira, T.K. Mondal, D. Ojha, A.M.Z. Slawin, E.R.T. Tiekink, A. Samanta, C. Sinha, Inorg. Chim. Acta 370 (2011) 175.
[39] B. Valuer, Molecular Fluorescence. Principles and Applications, Wiley-VCH, Weinheim, 2001.
[40] A.D. Becke, J. Chem. Phys. 98 (1993) 5648.
[41] C. Lee, W. Yang, R.G. Parr, Phys. Rev. B 37 (1988) 785.
[42] D. Andrae, U. Haeussermann, M. Dolg, H. Stoll, H. Preuss, Theor. Chim. Acta 77 (1990) 123.
[43] P. Fuentealba, H. Preuss, H. Stoll, L.V. Szentpaly, Chem. Phys. Lett. 89 (1989) 418.
[44] GAUSSIAN 03, Revision D.01, M.J. Frisch, G.W. Trucks, H.B. Schlegel, G.E. Scuseria, M.A. Robb, J.R. Cheeseman, J.A. Montgomery Jr., T. Vreven, K.N. Kudin, J.C. Burant, J.M. Millam, S.S. Iyengar, J. Tomasi, V. Barone, B. Mennucci, M. Cossi, G. Scalmani, N. Rega, G.A. Petersson, H. Nakatsuji, M. Hada, M. Ehara, K. Toyota, R. Fukuda, J. Hasegawa, M. Ishida, T. Nakajima, Y. Honda, O. Kitao, H. Nakai, M. Klene, X. Li, J.E. Knox, H.P. Hratchian, J.B. Cross, V. Bakken, C. Adamo, J. Jaramillo, R. Gomperts, R.E. Stratmann, O. Yazyev, A.J. Austin, R. Cammi, C. Pomelli, J.W. Ochterski, P.Y. Ayala, K. Morokuma, G.A. Voth, P. Salvador, J. J. Dannenberg, V. G. Zakrzewski, S. Dapprich, A.D. Daniels, M.C. Strain, O. Farkas, D.K. Malick, A.D. Rabuck, K. Raghavachari, J.B. Foresman, J.V. Ortiz, Q. Cui, A.G. Baboul, S. Clifford, J. Cioslowski, B.B. Stefanov, G. Liu, A. Liashenko, P. Piskorz, I. Komaromi, R.L. Martin, D.J. Fox, T. Keith, M.A. Al-Laham, C.Y. Peng, A.

Nanayakkara, M. Challacombe, P.M.W. Gill, B. Johnson, W. Chen, M.W. Wong, C. Gonzalez, J.A. Pople, Gaussian, Inc., Wallingford, CT, 2004.
[45] R. Bauernschmitt, R. Ahlrichs, Chem. Phys. Lett. 256 (1996) 454.
[46] R.E. Stratmann, G.E. Scuseria, M.J. Frisch, J. Chem. Phys. 109 (1998) 8218.
[47] M.E. Casida, C. Jamorski, K.C. Casida, D.R. Salahub, J. Chem. Phys. 108 (1998) 4439.
[48] V. Barone, M. Cossi, J. Phys. Chem. A 102 (1998) 1995.
[49] M. Cossi, V. Barone, J. Chem. Phys. 115 (2001) 4708.
[50] M. Cossi, N. Rega, G. Scalmani, V. Barone, J. Comput. Chem. 24 (2003) 669.
[51] N.M. O'Boyle, A.L. Tenderholt, K.M. Langner, J. Comput. Chem. 29 (2008) 839.
[52] SHELXS97: G.M. Sheldrick, SHELX97, Programs for Crystal Structure Analysis (release 97–2), University of Göttingen, Göttingen, Germany, 1997.
[53] SHELXL97: G.M. Sheldrick, SHELXL97, Programs for Crystal Structure Analysis (release 97–2), University of Göttingen, Göttingen, Germany, 1997.
[54] V.W.-W. Yam, V.C.-Y. Lau, L.-X. Wu, Dalton Trans. (1998) 1461.
[55] P. Kurz, B. Probst, B. Spingler, R. Alberto, Eur. J. Inorg. Chem. (2006) 2966.
[56] B. Machura, A. Świtlicka, I. Nawrot, K. Michalik, Inorg. Chem. Commun. 13 (2010) 1317.
[57] B. Machura, R. Kruszynski, J. Kusz, Polyhedron 26 (2007) 2543.